

Cite this: *Chem. Sci.*, 2026, 17, 5249

All publication charges for this article have been paid for by the Royal Society of Chemistry

Received 11th December 2025  
Accepted 15th January 2026

DOI: 10.1039/d5sc09734g

rsc.li/chemical-science

# Water-enhanced electrochemical hydrogenolysis of aryl C–O bonds

Yingying Pan, Jing Chen, Jie Li and Xuefeng Tan \*

Phenolic compounds are naturally abundant and easily derived, yet the cleavage of aryl C–O bonds typically relies on specific methods, especially those involving transition metal catalysts. In this study, we present a user-friendly and sustainable electrochemical approach for aryl C–O bond cleavage and hydrogenation. Salient features of this method include the use of an undivided cell, inexpensive dimethylformamide as a hydrogen source, a broad substrate scope, and practical derivatizations. A key factor in the success of this approach is the addition of water, which acts as a decomposing agent for the iminium intermediate, potentially competing with the substrate in cathodic reduction. Mechanistic studies elucidate the reaction cycle, with particular emphasis on the one-electron reduction process and the role of bromide.

## Introduction

Phenols are derived from a wide range of sources, including various natural products in plants, lignin breakdown products, and industrial processes involving coal tar and petroleum.<sup>1,2</sup> The hydroxyl group in phenols can direct numerous modifications due to its resonance effect, which makes the *ortho*- and *para*-positions on the aromatic ring electron-rich.<sup>3</sup> Given the abundance of phenolic compounds, transforming the hydroxyl group into other functional groups is of significant importance. However, the high bond dissociation energy (BDE) of the C–O bond in phenols (e.g., 112.4 kcal mol<sup>-1</sup> for phenol)<sup>4</sup> compared to the C–X bond in phenyl halides (e.g., 84 kcal mol<sup>-1</sup> for bromobenzene) poses a challenge for direct C–O bond cleavage in phenols.<sup>5–9</sup> To address this challenge, an activating group is typically introduced to the hydroxyl group to polarize the C–O bond, thereby facilitating subsequent C–O bond cleavage and transformations (Fig. 1a).<sup>10</sup>

Electrochemical organic synthesis utilizes electric potential as the driving force and electron transfer as the redox reagent, making it a green and sustainable synthetic technique.<sup>11–14</sup> This traditional synthetic tool has experienced a renaissance in recent years, with significant progress being made.<sup>15–29</sup> However, among these advancements, electrochemically driven C–O bond transformations have been relatively underexplored, especially for aryl C–O bonds.<sup>30–39</sup>

Two general strategies can be identified for electrochemical aryl C–O cleavage: electrochemical reduction and oxidation-initiated processes (Fig. 1b and c).<sup>33</sup> The first strategy involves installing an activating group on the hydroxyl group, such as

a triflate (Tf) or phosphate (Fig. 1b). Although the -OTf group is widely used as a halide analogue in chemical transformations, its electrochemical behavior differs significantly from that of halides in related compounds.<sup>40</sup> Under electrolysis, the S=O is prone to be reduced, leading to the S–O cleavage and formation of the starting phenol. Consequently, only indirect electrolysis,

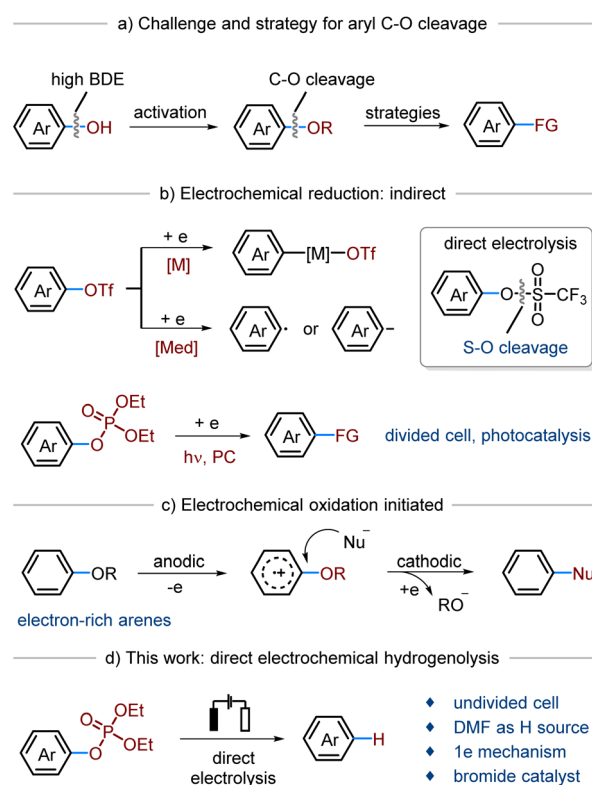


Fig. 1 Introduction of electrochemical aryl C–O cleavage.

Department of Chemistry, City University of Hong Kong, Tat Chee Avenue 83, Kowloon, Hong Kong SAR, 999077, China. E-mail: xuefetan@cityu.edu.hk



involving a redox-active transition metal catalyst,<sup>41–44</sup> or an organo-mediator,<sup>40</sup> can be successfully employed. For the phosphate activating group, the Wickens group has developed an electrochemical method that combines a photosensitizer to achieve aryl C–O cleavage and functionalization.<sup>45</sup> Although direct electrochemical electrolysis has been explored, the use of a divided cell setup presents operational challenges.<sup>46</sup> The first strategy is more prevalent due to its applicability to various phenolic substrates with different electronic properties. In contrast, the second strategy, recently disclosed by the Qiu group, is primarily suitable for electron-rich substrates (Fig. 1c).<sup>47</sup>

Based on the analysis above, electricity-driven aryl C–O cleavage remains underdeveloped, necessitating more general and practical strategies. In this work, we present an electrochemical method for aryl C–O cleavage and hydrogenation. Key features of our approach include: (1) the use of a practical undivided cell, (2) DMF as an inexpensive hydrogen source, and (3) mechanistic studies that reveal a unique single-electron reduction process and an important role of bromide.

## Results and discussion

We began our study by evaluating different activating groups on 4-phenylphenol (**1**) under electrochemical conditions (Fig. 2a). Initially, we selected a sacrificial iron anode and a lead cathode as electrodes, using <sup>n</sup>Bu<sub>4</sub>NBr as the electrolyte and dimethylformamide (DMF) as the solvent for electrolysis, in an undivided cell. The results show that different activating groups exhibit distinct chemoselectivity. Only the phosphate ester

yielded the desired aryl C–O cleavage product **2a**, while other groups resulted in the formation of the phenol product **3a**. We then considered replacing the sacrificial iron anode with other inexpensive and readily available chemical reducing agents, such as triethylamine (see the SI). To our delight, the desired product was observed even without any chemical reducing agent, although with a relatively low yield (around 50%). Monitoring the reaction profile revealed that the reaction nearly stops after 2 F mol<sup>-1</sup> of electricity is passed (Fig. 2b), suggesting the formation of a short-circuit cycle in the electrochemical system at a later stage. Considering anodic oxidation, two possible processes could be involved in the short-circuit cycle: the electrochemical redox process of Br<sup>-</sup>/Br<sub>2</sub> or DMF/iminium (Shono oxidation).<sup>48</sup> Since <sup>n</sup>Bu<sub>4</sub>NBF<sub>4</sub> also provides a moderate yield of **2a** while maintaining a steady cell voltage, it is more likely that the DMF/iminium redox cycle causes the short-circuit issue (Fig. 2c). A conceivable scenario is that DMF serves as a reducing agent and is oxidized to form an iminium intermediate. Over time, the accumulated iminium salt may compete with **1a** for cathodic reduction. Based on this assumption, we hypothesized that adding water might help degrade the iminium salt to hydrated formaldehyde, which is less reducible. To test this hypothesis, we added H<sub>2</sub>O as an additive (Fig. 2d). Indeed, under conditions identical to those in Fig. 2b, the addition of H<sub>2</sub>O significantly enhanced the yield of **2a** (entry 1). Varying the amount of electricity and current revealed that the optimal conditions are 70 mA and 4 F mol<sup>-1</sup> of electricity (entries 2–6).

With the optimal conditions established, we proceeded to examine the substrate scope for electrochemical aryl C–O

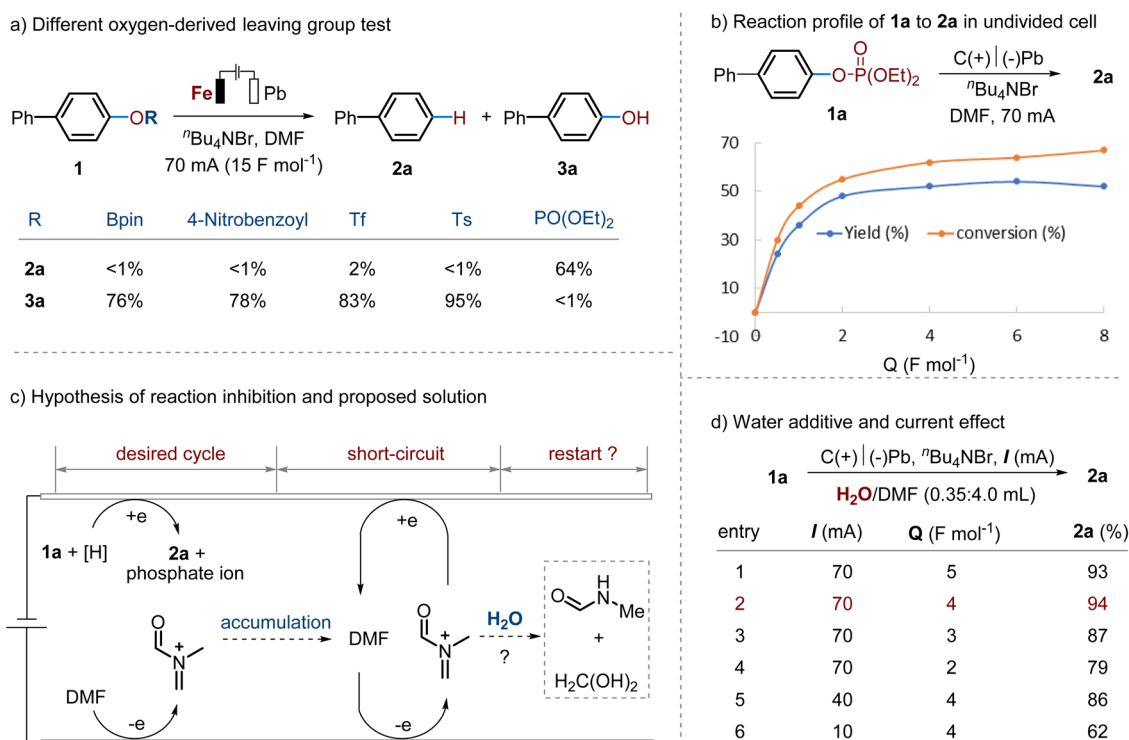


Fig. 2 Reaction condition optimization for the electrochemical hydrogenolysis of **1a**.



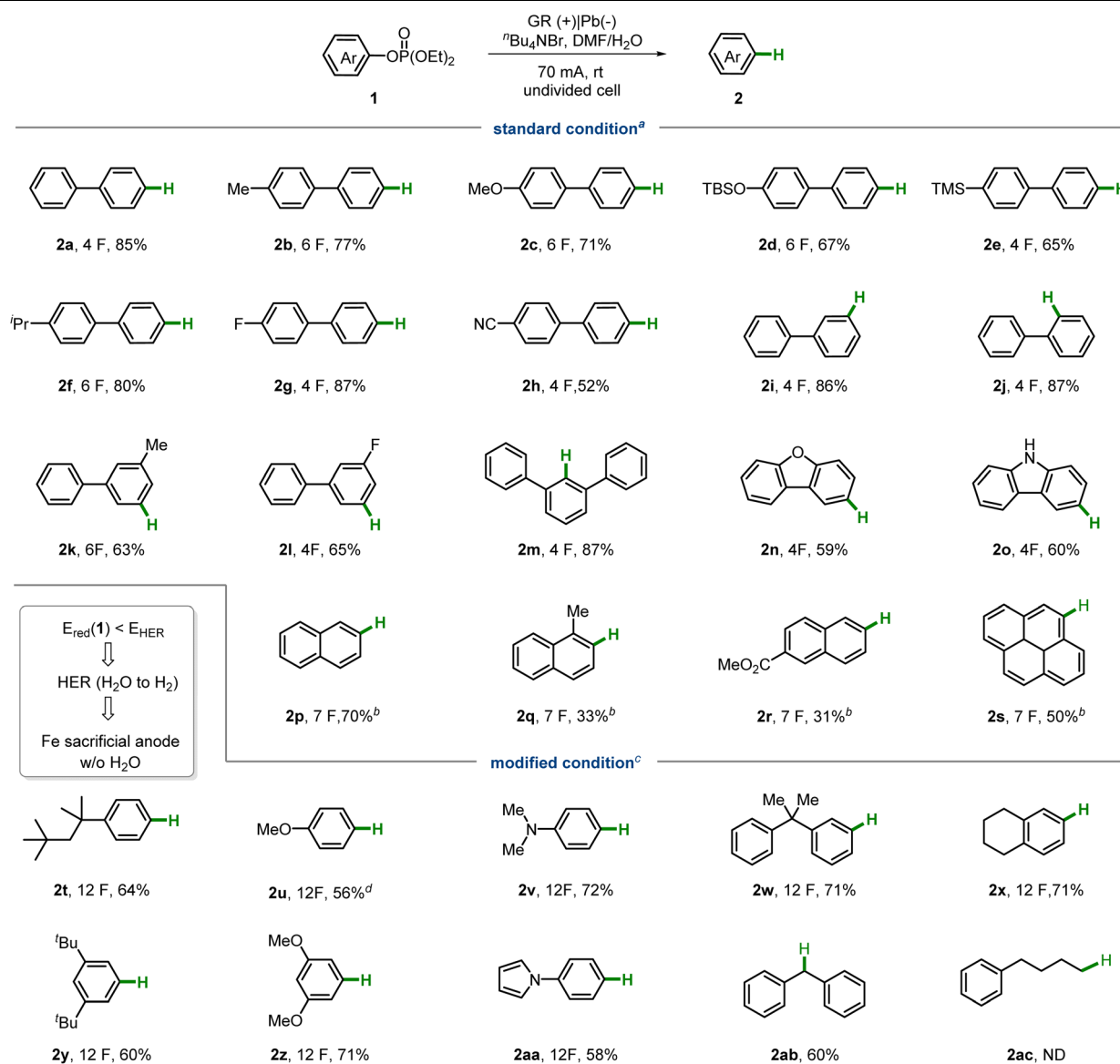
hydrogenolysis (Table 1). Biphenyl backbones bearing various functional groups at different positions were well-tolerated (**2a–m**). Both electron-donating groups, such as methyl (**2b**), methoxyl (**2c**), and trimethylsilyl (**2e**), and electron-withdrawing groups, such as fluoro (**2g**) and nitrile (**2h**), were compatible. Additionally, substrates based on dibenzofuran and carbazole (**2n–o**) were suitable for the system.

Naphthalene-derived phenols proved too reactive under standard conditions, often leading to over-reduction of the naphthalene ring. To mitigate this side reaction, we applied a slight modification to the standard conditions, using a lower current (20 mA) and omitting the water additive for naphthyl-

based phosphate esters (**2p–s**). As a result, only moderate yields were achieved for these substrates.

While adding water can alleviate the competing reduction of the potential iminium intermediate, it also increases the risk of the hydrogen evolution reaction (HER) at the cathode. This issue is particularly significant for substrates with high reduction potentials, where HER may outcompete the desired substrate reduction. Indeed, monophenyl ring-based substrates face this challenge and cannot be effectively reduced under standard conditions. Consequently, we applied a modified condition featuring a sacrificial iron anode and no water additive for monophenyl ring-based substrates (Table 1, **2t–2ac**). A

Table 1 Substrate scope<sup>a</sup>



<sup>a</sup> Standard conditions: **1** (0.40 mmol), <sup>n</sup>Bu<sub>4</sub>NBr (1.0 equiv.), DMF/H<sub>2</sub>O (4.0 : 0.35 mL), GR anode (10 mm × 10 mm × 0.5 mm) and lead cathode (10 mm × 10 mm × 0.5 mm), 70 mA (4.0–6.0 F mol<sup>-1</sup>), rt, isolated yields. <sup>b</sup> Same as standard conditions, except without the addition of H<sub>2</sub>O, 20 mA, 4 h (7.0 F mol<sup>-1</sup>), 50 °C. <sup>c</sup> Modified conditions: **1** (0.40 mmol), <sup>n</sup>Bu<sub>4</sub>NBr (1.0 equiv.), DMF (4 mL), Fe anode (10 mm × 10 mm × 0.2 mm) and lead cathode (10 mm × 10 mm × 0.5 mm), 70 mA, 2 h (12.0 F mol<sup>-1</sup>), rt. <sup>d</sup> Yield was determined by GC using dodecane as internal standard.



diverse range of substituents, such as alkyl (**2t**, **2w–y**), methoxyl (**2u** and **2z**), amino (**2v**), and pyrrole (**2aa**), were compatible with these conditions. Interestingly, the benzylic alcohol-based substrate (**2ab**) was suitable, while the non-benzylic alkyl-based substrate (**2ac**) was non-reducible. Unfortunately, aside from the fluorine atom, other halides like chlorine and bromine are not tolerated under either condition, resulting primarily in C–X bond cleavage.

Phenolic compounds are naturally abundant and easily derived, and when combined with our electrochemical aryl C–O cleavage, the hydroxyl group can serve as a traceless directing group. To demonstrate this concept, we conducted several derivatizations to showcase the directing capability of the hydroxyl group and the robustness of our electrochemical method (Fig. 3). In the first example, we illustrate the facile bromination of phenol at the *ortho*- and *para*-positions, followed by Suzuki coupling and phosphate esterification to produce compound **4** (Fig. 3a). Compound **4** undergoes smooth hydrogenolysis under our standard electrochemical conditions, yielding 1,3,5-triaryl substituted benzene **5**, which is often used in the synthesis of cage molecules.<sup>49</sup> The second example starts with commercially inexpensive (*R*)-BINOL, which is methylated and esterified with phosphate chloride to form compound **6**. This compound can be selectively deoxygenated

electrochemically to produce compound **7** (Fig. 3b). We were pleased to observe that product **7** did not undergo significant racemization under the electrochemical conditions. *L*-Tyrosine, a naturally occurring amino acid with a phenol motif, was employed to harness the directing ability of the hydroxyl group, allowing us to introduce a phenyl group adjacent to the hydroxyl group (Fig. 3c). When the modified tyrosine derivative **8** was subjected to our electrochemical deoxygenation, a modified phenylalanine derivative **9** was effectively prepared. Notably, the N–OMe group was cleaved under these electrochemical conditions. This method demonstrates the potential for synthesizing unnatural amino acids from natural ones. Finally, we demonstrated hydroxyl group-directed Friedel–Crafts alkylation of compound **10** to prepare compound **11**. Compound **11** can be effectively deoxygenated under modified conditions to yield compound **12**, which serves as a valuable synthon for the production of CB1 cannabinoid receptors.<sup>50</sup>

Next, we explored the reaction mechanism, specifically focusing on how DMF functions as a reducing agent and why the addition of water enhances reaction efficiency. To investigate this, we replaced H<sub>2</sub>O with deuterium water (D<sub>2</sub>O) under standard conditions and observed a 23% deuterium incorporation in the product (Fig. 4a). This observation suggests the involvement of a minor carbanion intermediate. Since

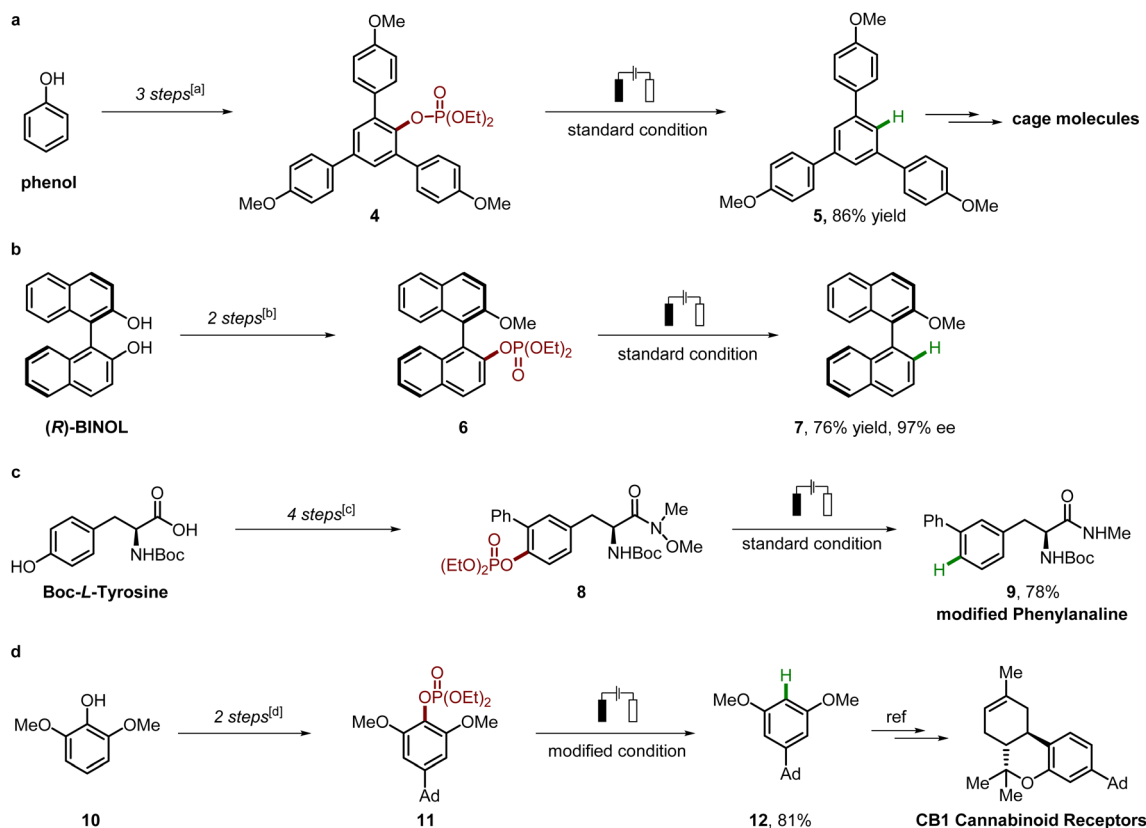


Fig. 3 Applications of the electrochemical hydrogenolysis. <sup>a</sup>Step 1: NBS, THF, 0 °C to rt, 16 h; step 2: Pd(PPh<sub>3</sub>)<sub>4</sub>, 4-OMePhBS(OH)<sub>2</sub>, K<sub>2</sub>CO<sub>3</sub>, DMF, 100 °C, 4 h; step 3: ClPO(OEt)<sub>2</sub>, NEt<sub>3</sub>, DCM, rt, overnight; <sup>b</sup>step 1: K<sub>2</sub>CO<sub>3</sub>, MeI, acetone, reflux, overnight; step 2: ClPO(OEt)<sub>2</sub>, NEt<sub>3</sub>, DCM, rt, overnight; <sup>c</sup>step 1: MeNHOMe HCl, HATU, DIPEA, DMF, rt, 10 min; step 2: NIS, TsOH H<sub>2</sub>O, MeOH, rt, 10 min; step 3: Pd(PPh<sub>3</sub>)<sub>4</sub>, PhB(OH)<sub>2</sub>, K<sub>2</sub>CO<sub>3</sub>, DMF, 100 °C, 4 h; step 4: ClPO(OEt)<sub>2</sub>, NEt<sub>3</sub>, DCM, rt, overnight; <sup>d</sup>step 1: methanesulfonic acid, 1-adamantanol, DCM, rt, overnight; step 2: ClPO(OEt)<sub>2</sub>, NEt<sub>3</sub>, DCM, rt, overnight.



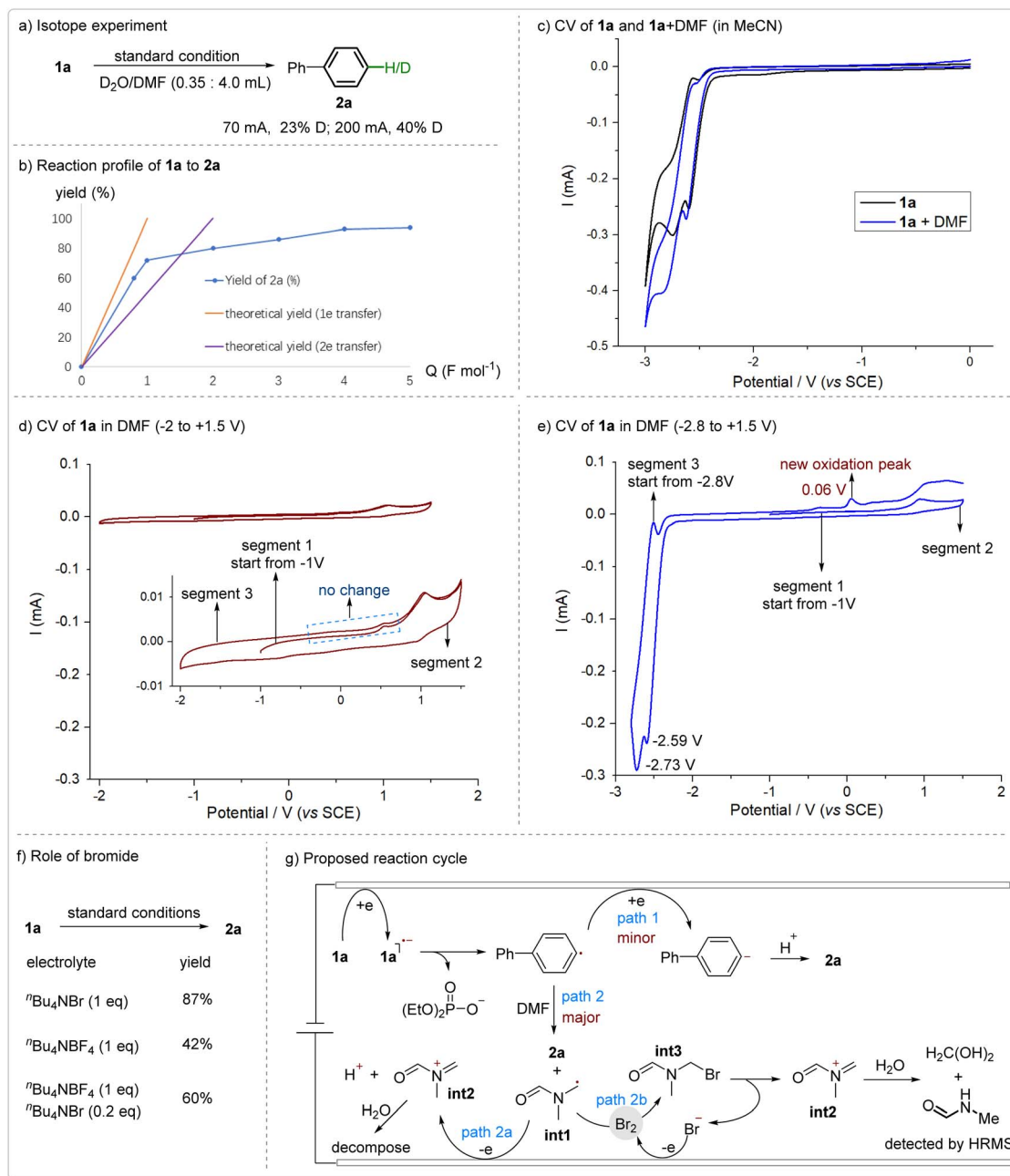


Fig. 4 Mechanistic studies.

carbanions result from a two-electron reduction, increasing electron density could potentially lead to more carbanion formation. Indeed, higher currents resulted in increased deuterium incorporation, indicating an enhanced two-electron reduction pathway (Fig. 4a). This experiment also supports the fact that the primary pathway involves a one-electron reduction, yielding a radical intermediate. Additionally, by measuring the reaction profile of **1a** to **2a** under standard conditions, we found that the reaction initially occurs in a zone between one-electron and two-electron processes, suggesting a strong likelihood of a one-electron pathway (Fig. 4b).

Once **1a** is reduced to generate a radical intermediate, it is highly likely that DMF transfers a hydrogen atom to this radical.

This scenario was confirmed by cyclic voltammetry (CV) studies (Fig. 4c). Adding DMF to **1a** induced a catalytic current at the reduction peaks of **1a**, indicating a reaction between DMF and the reduced intermediate of **1a**. Further CV studies scanned **1a** in DMF across different potential ranges (−2 V to 1.5 V, Fig. 4d; and −2.8 V to 1.5 V, Fig. 4e). Three segments with specific scanning directions (−1.0 V → +1.5 V → −2.0/−2.8 V → +1.5 V) were conducted (Fig. 4d and e). Within the range of −2.0 V to 1.5 V, the first and third segments remained unchanged, indicating no formation of new species. In contrast, within the range of −2.8 V to 1.5 V, a new oxidation peak ( $E_p = +0.06$  V) appeared in the third segment, suggesting that the reduction ( $E_p = -2.59$  or  $-2.73$  V) induced the generation of new species,



likely DMF-related radical species. Considering the difficulty of direct electrochemical oxidation of DMF ( $E_{\text{onset}} > +1.7$  V vs. SCE, see SI), the anodic oxidation of this newly generated species is more feasible, making the undivided-cell setup viable. In summary, although DMF has weak reducing ability, the cathodic reduction enhances its reducibility through radical formation.

However, given the typically short-lived nature of radical species, it is unlikely that the DMF radical can diffuse through the solvent and travel to the anode for oxidation. Instead, it is more plausible that the radical species is stabilized or indirectly oxidized upon generation. With this thought in mind, we observed that the bromide-containing electrolyte,  ${}^n\text{Bu}_4\text{NBr}$ , is more effective in supporting the reaction than  ${}^n\text{Bu}_4\text{NBF}_4$ , even in catalytic amounts (Fig. 4f). Moreover, bromide has a low oxidation potential ( $E_{\text{onset}} = +0.6$  V vs. SCE, see SI), which is slightly higher than that of the newly generated species but significantly lower than that of DMF. In this context, we strongly speculate that  $\text{Br}^-$  may act as a mediator, facilitating the anodic oxidation of the DMF radical (see details in the proposed mechanism, Fig. 4g).

Finally, a plausible mechanistic cycle is illustrated in Fig. 4g. The substrate **1a** undergoes cathodic reduction to yield either an aryl radical (*via* a one-electron reduction) or a carbanion (*via* a two-electron reduction), with the aryl radical pathway being predominant. While the carbanion can be directly protonated to form product **2a** (path 1), the aryl radical intermediate can abstract a hydrogen atom from DMF to generate radical species **int1** (path 2). **int1** can be oxidized either directly at the anode (path 2a) or indirectly *via* mediation by  $\text{Br}^-$  (path 2b), leading to the formation of an iminium salt. Path 2b is more favored due to the observed advantageous role of  $\text{Br}^-$ . Upon the addition of water, the iminium salt decomposes to yield non-reducible hydrated formaldehyde and methylformamide, which can be detected by HRMS (see SI).

## Conclusions

In conclusion, we have developed an electrochemical hydrogenolysis method for phenolic phosphate esters. This approach is characterized by its user-friendly undivided cell setup, the use of inexpensive DMF as a hydrogen source, and a broad substrate scope. The successful implementation of the undivided cell is facilitated by the addition of water, which helps mitigate competitive and undesired cathodic reduction reactions. Mechanistic studies revealed that this process primarily involves one-electron reduction, featuring cathodic reduction-enhanced anodic oxidation. We also explored the subtle effect of bromide, proposing its likely involvement in the mechanism. In summary, this work unveils a refined electrochemical process for aryl C–O cleavage under mild and general conditions, potentially guiding future research in related areas.

## Author contributions

Y. P. performed and developed the reaction, conducted the majority of the substrate scope and mechanistic studies. J. C.

and J. L. contributed to the substrate synthesis and data analysis. X. T. conceptualized and directed the project. Y. P and X. T. drafted the manuscript. All authors contributed to the discussions.

## Conflicts of interest

The authors declare no conflict of interest.

## Data availability

All data supporting this article are available as part of the article and its supplementary information (SI). Supplementary information is available. See DOI: <https://doi.org/10.1039/d5sc09734g>.

## Acknowledgements

This work was supported by the Hong Kong Research Grants Council (21304324) and start-up fund from the City University of Hong Kong (Project no 9610667) for financial support.

## Notes and references

- B. R. Albuquerque, S. A. Heleno, M. B. P. P. Oliveira, L. Barros and I. C. F. R. Ferreira, *Food Funct.*, 2021, **12**, 14–29.
- V. Cheyner, *Phytochem. Rev.*, 2012, **11**, 153–177.
- Z. Rappoport, *The chemistry of phenols*, John Wiley & Sons, 2004.
- S. J. Blanksby and G. B. Ellison, *Acc. Chem. Res.*, 2003, **36**, 255–263.
- J. Zhang, J. Sun and Y. Wang, *Green Chem.*, 2020, **22**, 1072–1098.
- Z. Qiu and C. J. Li, *Chem. Rev.*, 2020, **120**, 10454–10515.
- S. Kim, E. E. Kwon, Y. T. Kim, S. Jung, H. J. Kim, G. W. Huber and J. Lee, *Green Chem.*, 2019, **21**, 3715–3743.
- W. Jin, L. Pastor-Pérez, D. Shen, A. Sepúlveda-Escribano, S. Gu and T. Ramirez Reina, *ChemCatChem*, 2019, **11**, 924–960.
- Q. Bu, H. Lei, A. H. Zacher, L. Wang, S. Ren, J. Liang, Y. Wei, Y. Liu, J. Tang, Q. Zhang and R. Ruan, *Bioresour. Technol.*, 2012, **124**, 470–477.
- T. Zhou and M. Szostak, *Catal. Sci. Technol.*, 2020, **10**, 5702–5739.
- M. C. Leech, A. D. Garcia, A. Petti, A. P. Dobbs and K. Lam, *React. Chem. Eng.*, 2020, **5**, 977–990.
- A. Wiebe, T. Gieshoff, S. Möhle, E. Rodrigo, M. Zirbes and S. R. Waldvogel, *Angew. Chem., Int. Ed.*, 2018, **57**, 5594–5619.
- S. Möhle, M. Zirbes, E. Rodrigo, T. Gieshoff, A. Wiebe and S. R. Waldvogel, *Angew. Chem., Int. Ed.*, 2018, **57**, 6018–6041.
- K. D. Moeller, *Chem. Rev.*, 2018, **118**, 4817–4833.
- Y. Wang, S. Dana, H. Long, Y. Xu, Y. Li, N. Kaplaneris and L. Ackermann, *Chem. Rev.*, 2023, **123**, 11269–11335.
- Y. Liu, P. Li, Y. Wang and Y. Qiu, *Angew. Chem., Int. Ed.*, 2023, **62**, e202306679.
- X. Cheng, A. Lei, T.-S. Mei, H. C. Xu, K. Xu and C. Zeng, *CCS Chem.*, 2022, **4**, 1120–1152.



- 18 N. E. S. Tay, D. Lehnerr and T. Rovis, *Chem. Rev.*, 2022, **122**, 2487–2649.
- 19 S.-H. Shi, Y. Liang and N. Jiao, *Chem. Rev.*, 2021, **121**, 485–505.
- 20 L. F. T. Novaes, J. Liu, Y. Shen, L. Lu, J. M. Meinhardt and S. Lin, *Chem. Soc. Rev.*, 2021, **50**, 7941–8002.
- 21 C. Ma, P. Fang, Z.-R. Liu, S.-S. Xu, K. Xu, X. Cheng, A. Lei, H. C. Xu, C. Zeng and T.-S. Mei, *Sci. Bull.*, 2021, **66**, 2412–2429.
- 22 K. Yamamoto, M. Kuriyama and O. Onomura, *Acc. Chem. Res.*, 2020, **53**, 105–120.
- 23 Q. Jing and K. D. Moeller, *Acc. Chem. Res.*, 2020, **53**, 135–143.
- 24 P. Xiong and H.-C. Xu, *Acc. Chem. Res.*, 2019, **52**, 3339–3350.
- 25 H. Wang, X. Gao, Z. Lv, T. Abdelilah and A. Lei, *Chem. Rev.*, 2019, **119**, 6769–6787.
- 26 J.-i. Yoshida, A. Shimizu and R. Hayashi, *Chem. Rev.*, 2018, **118**, 4702–4730.
- 27 J. E. Nutting, M. Rafiee and S. S. Stahl, *Chem. Rev.*, 2018, **118**, 4834–4885.
- 28 M. Yan, Y. Kawamata and P. S. Baran, *Chem. Rev.*, 2017, **117**, 13230–13319.
- 29 R. Francke and R. D. Little, *Chem. Soc. Rev.*, 2014, **43**, 2492–2521.
- 30 Y.-X. Zheng, Y.-X. Wu, L.-J. Su, P. Xiong and H.-C. Xu, *Angew. Chem., Int. Ed.*, 2025, **64**, e202509411.
- 31 Y.-X. Zheng, Y. Gao, P. Xiong and H.-C. Xu, *Angew. Chem., Int. Ed.*, 2025, **64**, e202423241.
- 32 L. Yu, S. Li, H. Ogawa, Y. Ma, Q. Chen, K. Yamazaki, Y. Nagata and H. Nakamura, *Nat. Commun.*, 2025, **16**, 8379.
- 33 A. J. Ressler, J. I. Martinez Alvarado, R. Hariharan, W. Guan and S. Lin, *Angew. Chem., Int. Ed.*, 2025, **64**, e202510069.
- 34 X. Guo, N. G. Price and Q. Zhu, *Org. Lett.*, 2024, **26**, 7347–7351.
- 35 Q. Guo, Y. Jiang, R. Zhu, W. Yang and P. Hu, *Angew. Chem., Int. Ed.*, 2024, **63**, e202402878.
- 36 P. Villo, A. Shatskiy, M. D. Kärkäs and H. Lundberg, *Angew. Chem., Int. Ed.*, 2023, **62**, e202211952.
- 37 W. Guan, Y. Chang and S. Lin, *J. Am. Chem. Soc.*, 2023, **145**, 16966–16972.
- 38 C. Huang, W. Ma, X. Zheng, M. Xu, X. Qi and Q. Lu, *J. Am. Chem. Soc.*, 2022, **144**, 1389–1395.
- 39 Z. Li, W. Sun, X. Wang, L. Li, Y. Zhang and C. Li, *J. Am. Chem. Soc.*, 2021, **143**, 3536–3543.
- 40 X. Kong, Y. Chen, X. Chen, C. Ma, M. Chen, W. Wang, Y.-Q. Xu, S.-F. Ni and Z.-Y. Cao, *Nat. Commun.*, 2023, **14**, 6933.
- 41 A. Jutand and S. Négri, *Eur. J. Org. Chem.*, 1998, **1998**, 1811–1821.
- 42 A. Jutand and S. Négri, *Synlett*, 1997, **1997**, 719–721.
- 43 A. Jutand and A. Mosleh, *J. Org. Chem.*, 1997, **62**, 261–274.
- 44 A. Jutand, S. Négri and A. Mosleh, *J. Chem. Soc., Chem. Commun.*, 1992, 1729–1730.
- 45 X. Tian, T. A. Karl, S. Reiter, S. Yakubov, R. de Vivie-Riedle, B. König and J. P. Barham, *Angew. Chem., Int. Ed.*, 2021, **60**, 20817–20825.
- 46 T. Shono, Y. Matsumura, K. Tsubata and Y. Sugihara, *J. Org. Chem.*, 1979, **44**, 4508–4511.
- 47 S. Chen, A. Shi, G. Yang, P. Xie, F. Liu and Y. Qiu, *Chin. Chem. Lett.*, 2025, **36**, 110810.
- 48 J. Y. Becker, *Chemelectrochem*, 2024, **11**, e202400023.
- 49 N. Lin, R. Xie, H. Jia and Y. Chen, *Org. Lett.*, 2025, **27**, 1853–1857.
- 50 D. Lu, Z. Meng, G. A. Thakur, P. Fan, J. Steed, C. L. Tartal, D. P. Hurst, P. H. Reggio, J. R. Deschamps, D. A. Parrish, C. George, T. U. C. Järbe, R. J. Lamb and A. Makriyannis, *J. Med. Chem.*, 2005, **48**, 4576–4585.

